SECURITY CLASSIFICATION OF THIS PAGE

REPORT DOCUMENTATION PAGE

1a REPORT SECURITY CLASSIFICATION UNCLASSIFIED	1b. RESTRICTIVE MARKINGS
2a SECURITY CLASSIFICATION AUTHORITY 2b DECLASSIFICATION / DOWNGRADING SCHEDULE	3 DISTRIBUTION / AVAILABILITY OF REPORT Approved for public release; distribution unlimited.
4 PERFORMING ORGANIZATION REPORT NUMBER(S) NRL Report 8871	5. MONITORING ORGANIZATION REPORT NUMBER(S)
6a. NAME OF PERFORMING ORGANIZATION Naval Research Laboratory 6b OFFICE SYMBOL *(If applicable)*	7a. NAME OF MONITORING ORGANIZATION
6c. ADDRESS *(City, State, and ZIP Code)* Washington, DC 20375-5000	7b. ADDRESS *(City, State, and ZIP Code)*
8a. NAME OF FUNDING / SPONSORING ORGANIZATION Office of Naval Research 8b. OFFICE SYMBOL *(If applicable)*	9. PROCUREMENT INSTRUMENT IDENTIFICATION NUMBER
8c. ADDRESS *(City, State, and ZIP Code)* Arlington, VA 22217	10. SOURCE OF FUNDING NUMBERS PROGRAM ELEMENT NO: 61153N; PROJECT NO.: 021-05-43; TASK NO.: 53; WORK UNIT ACCESSION NO.: DN480-006

11 TITLE *(Include Security Classification)*
Rational Pulse-Shaping Filters for Almost MSK-Like Modulation

12 PERSONAL AUTHOR(S)
Coleman, J. O.

13a. TYPE OF REPORT	13b. TIME COVERED	14. DATE OF REPORT *(Year, Month, Day)*	15. PAGE COUNT
Interim	FROM 5/81 TO 10/84	1985 March 22	34

16 SUPPLEMENTARY NOTATION

17 COSATI CODES			18. SUBJECT TERMS *(Continue on reverse if necessary and identify by block number)*
FIELD	GROUP	SUB-GROUP	Minimum-shift keying; Pulse compression; Digital communication; MSK modulation

19 ABSTRACT *(Continue on reverse if necessary and identify by block number)*

MSK-like data-modulation formats are those for which: (a) the instantaneous phase of the transmitted signal changes by exactly 90° in each bit interval; (b) the envelope of the transmitted signal is constant; and (c) the power spectrum of the transmitted signal rolls off asymptotically faster than the spectrum of ordinary (rectangular or unfiltered) QPSK. Well-known members of this family include MSK (minimum-shift keying), SFSK (sinusoidal frequency-shift keying), and DSFSK (doubly sinusoidal frequency-shift keying). These modulation types are well suited both to data communication and to radar pulse compression using binary code sequences. Unfortunately, most MSK-like formats have complex implementations. In this report, new modulation formats are described which come close to being in the MSK-like class, yet are inherently simple to implement using baseband pulse-shaping filters with low-order rational transfer functions.

20 DISTRIBUTION / AVAILABILITY OF ABSTRACT ☒ UNCLASSIFIED/UNLIMITED ☐ SAME AS RPT ☐ DTIC USERS	21. ABSTRACT SECURITY CLASSIFICATION UNCLASSIFIED
22a NAME OF RESPONSIBLE INDIVIDUAL M.I. Skolnik	22b TELEPHONE *(Include Area Code)* (202) 767-2936 22c. OFFICE SYMBOL 5300

DD FORM 1473, 84 MAR 83 APR edition may be used until exhausted
All other editions are obsolete

SECURITY CLASSIFICATION OF THIS PAGE

NRL Report 8871

Rational Pulse-Shaping Filters for Almost MSK-Like Modulation

J. O. COLEMAN

Radar Analysis Branch
Radar Division

March 22, 1985

NAVAL RESEARCH LABORATORY
Washington, D.C.

CONTENTS

RATIONAL PULSE-SHAPING FILTERS FOR ALMOST MSK-LIKE MODULATION

1. INTRODUCTION

MSK-like modulation formats are those for which (a) the instantaneous phase of the transmitted signal changes by exactly 90° in each bit interval, and (b) the instantaneous amplitude (or envelope) of the transmitted signal is constant. Well-known members of this family include MSK [1] (minimum-shift keying), SFSK (sinusoidal frequency-shift keying) [2], and DSFSK (doubly sinusoidal frequency-shift keying) [3]. These formats are used where a constant envelope is needed but with a sharper spectral rolloff than is provided by rectangular QPSK (quadriphase-shift keying). Rectangular QPSK rolls off asymptotically at 6 dB/octave, MSK rolls off at 12 dB/octave, SFSK at 24 dB/octave, and DSFSK at 36 dB/octave. The width of the main spectral lobe is greater for the formats with the sharper asymptotic spectral rolloffs. Of these formats, only MSK is easily generated, and consequently MSK is used regularly both for data communication and for radar pulse compression with binary-coded sequences. The other formats, desirable for their lower spectral sidelobes, generally require complex filters or precision voltage-controlled oscillators, making them difficult to implement, or rely on digital signal-generation methods, making them unsuitable for high-speed operation.

In this report, simple implementations are sought not by looking for simple approximations to existing modulation formats in the MSK-like class, but by searching within a particular easily implemented class for those modulation formats that come *closest* to being MSK-like. This approach resulted in several new modulation formats that (a) change phase by 90° in each bit interval; (b) have *almost* constant envelope; and (c) can be implemented to good approximation using low-order rational transfer functions to filter in-phase and quadrature NRZ (nonreturn-to-zero) waveforms. These new formats were derived by first starting with the class of waveforms that can be generated by passing in-phase and quadrature NRZ waveforms through identical filters with rational transfer functions, modulating the two waveforms onto quadrature carriers, and summing. Further restricting the class of waveforms considered to those that change phase by 90° in each bit interval, the locations of the singularities of the transfer functions of the pulse-shaping filters were optimized with respect to the mean of the fourth power of the signal amplitude with signal energy constrained to be constant. This resulted in modulation formats with very small variations in amplitude.

If small amplitude fluctuations were not present, these modulation formats would be MSK-like. I use the term *almost MSK-like* to refer to modulation formats, such as those presented here, that have such small amplitude variations that they can be treated as MSK-like for all practical purposes. I refer to the optimum almost-MSK-like modulation formats presented in this report as *RSK,* for *rational-shift keying.* The term *rational* emphasizes that these formats, unlike the MSK-like formats, can be generated with rational pulse-shaping filters. The *-shift keying* emphasizes the similarity to the MSK-like formats. The term is more mnemonic than accurate, however, for the instantaneous frequency shift of RSK signals cannot be described as a rational function. Nevertheless, I use the term RSK here for lack of a more descriptive, equally concise term. To differentiate between the various RSK formats described in this report I will use the order of the associated pulse-shaping filter. This report derives fourth-, sixth-, and eighth-order RSK formats.

Manuscript approved November 5, 1984.

The remainder of this report is organized into five sections. The section following this introduction establishes notation and provides the minimum background necessary to understand the remainder of the report. The class of modulation formats optimized is then developed. The optimization criterion used to choose the best formats within that class is then presented, followed by a presentation of the RSK formats that resulted from the optimization process. The summary includes the RSK parameters in tabular format for convenient reference. Various lengthy mathematical details are relegated to appendixes.

2. BACKGROUND: QUADRATURE DATA-MODULATION FORMATS

In this section I describe several related modulation types as a vehicle for establishing notation. I first describe a very general modulation format, and then I describe various subsets of that format until I have described the class of modulation formats optimized in the following sections.

QAM

Consider amplitude modulating a carrier with a complex modulation function $m(t)$, where*

$$m(t) = i(t) + jq(t),$$

with $i(t)$ and $q(t)$ real, and

$$s_c(t) = \mathrm{Re}\{ m(t)\, e^{j\omega_c t}\} = i(t)\cos\omega_c t - q(t)\sin\omega_c t. \tag{1}$$

This is referred to as *quadrature amplitude modulation* or QAM. The complex modulation function $m(t)$ can be recovered from $s_c(t)$ if $m(t)$ is band-limited to frequencies $\omega > -\omega_c$. Conversely, any real $s_c(t)$ with no DC component can be generated with a suitable $m(t)$. Thus, QAM is a very general modulation format; all of the modulation formats discussed in this report are special forms of QAM.

QPSK

QPSK, or *quadriphase-shift keying,* is a form of QAM in which

$$m(t) = Ae^{j\phi} \sum_m \alpha_m p(t - 2mT), \tag{2}$$

with each $\alpha_m \in \{1, j, -1, -j\}$ and with $p(t)$, termed the *baseband pulse function,* satisfying

$$\eta p(d + 2kT) = \delta_k \tag{3}$$

(δ_k is the Kronecker delta function) for some fixed delay d and scale factor η. The latter condition is the time-domain equivalent of Nyquist's second criterion and is required to prevent intersymbol interference, i.e., to ensure that at times $t = d + 2kT$ only one term contributes to the sum in Eq. (2). If $p(t)$ is a rectangular pulse of width $2T$, so-called *rectangular* QPSK results. The term QPSK itself is reserved by some authors for rectangular QPSK.

QPSK is frequently used in data communication, where bits are made available for transmission at rate T^{-1}. Bits are grouped into pairs, and each pair is mapped into one of the α_m, with each of the four permutations of two bits mapped into one of the four possible values for the α_m. Rectangular QPSK is also occasionally used in radar pulse compression, where the quaternary sequence $\{\alpha_m\}$ is carefully chosen to have desirable autocorrelation properties. There is no reason why nonrectangular QPSK could not be used in pulse compression as long as the amplitude of the baseband pulse function $p(t)$ decayed quickly in either direction from the peak.

*The unit imaginary quantity is represented in this report by j rather than i. This is common in the literature of electrical engineering and here permits the conventional use of i for *in-phase.*

The conventional implementation of QPSK effectively rearranges Eq. (2) to obtain

$$m(t) = \left\{ \sum_m \alpha_m g(t - 2mT) \right\} \circledast f(t), \tag{4}$$

where $\circledast$ indicates convolution, and where $g(t) \circledast f(t) = p(t)$ of Eq. (2). The gate function $g(t)$ is defined by

$$g(t) = U(t) - U(t - 2T), \tag{5}$$

where $U(t)$ is the unit-step function, i.e., $g(t)$ is equal to unity for $0 \leqslant t < 2T$ and zero everywhere else. Thus, the bracketed sum in Eq. (4) is just a pair (real and imaginary parts) of NRZ digital waveforms. Since $f(t)$ is nearly always a purely real function, the QPSK implementation corresponding to this formulation is as shown in Fig. 1. The convolution of Eq. (4) is implemented by passing the two NRZ data streams derived from the α_m through pulse-shaping filters with impulse responses $f(t)$. The upper and lower signal paths in Fig. 1 are referred to respectively as either the *i* and *q* *channels* or *arms*. The pulse-shaping filters in the *i* and *q* channels are referred to in the remainder of this report by their conventional names, the *i* and *q* arm filters.

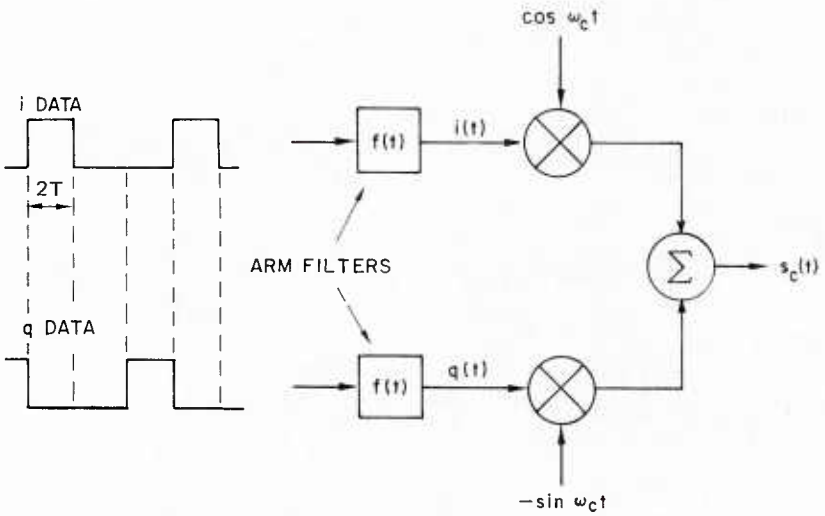

Fig. 1 — Conventional QPSK implementation

OQPSK

Attempts in the data-communication community to develop modulation formats less susceptible to degradation in nonlinear transmitters led to the development of *staggered* or *offset* QPSK, abbreviated OQPSK. OQPSK is identical to QPSK except that the imaginary part $q(t)$ of the modulation function $m(t)$ in Eq. (2) has been offset in time from the real part $i(t)$ by time T. This reduces the extreme envelope fluctuations in $s_c(t)$ of Eq. (1) suffered by ordinary QPSK (especially if nearly rectangular) whenever $\alpha_m = -\alpha_{m-1}$ in Eq. (2).

A mathematical formulation of OQPSK in terms of the $m(t)$ of Eq. (2) is clumsy. OQPSK is more concisely defined as QAM with

$$m(t) = \sum_m \beta_m j^m p(t - mT), \tag{6}$$

where each $\beta_m \in \{1,-1\}$, and where $p(t)$ is constrained as for ordinary QPSK above. The $\{\beta_m\}$ in Eq. (6) might typically be chosen for data transmission as

$$\beta_m = \begin{cases} \beta_{m-1} & \text{to send a 1} \\ -\beta_{m-1} & \text{to send a 0,} \end{cases} \tag{7}$$

where β_0 is chosen arbitrarily. OQPSK is not any less suited to radar pulse compression than ordinary QPSK.

The factor $Ae^{j\phi}$ of Eq. (2) was omitted in Eq. (6) in the interest of brevity. It should be understood that OQPSK and any of the modulation formats described subsequently can have an arbitrary amplitude-and-phase factor added.

The OQPSK formulation of Eq. (6) can also be rewritten to explicitly indicate the use of arm filters on NRZ data streams:

$$m(t) = \left\{ \sum_m \beta_m j^m g(t - mT) \right\} \circledast f(t). \tag{8}$$

The corresponding implementation is given in Fig. 2. The only difference between Figs. 2 and 1 is that in Fig. 2 the q data stream has been offset from the i data stream by time T. The data values fed to the arm filters in Fig. 2 are related in a simple way to the $\{\beta_m\}$ of Eq. (8), but the details are unimportant here.

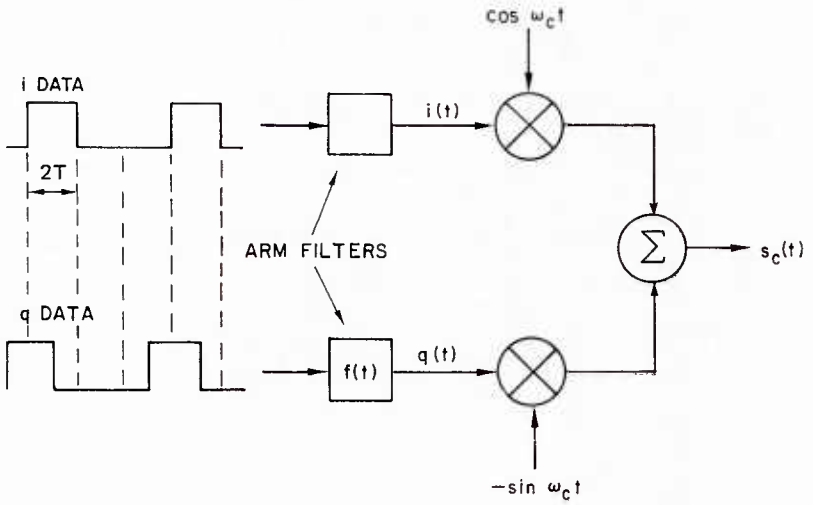

Fig. 2 — Conventional offset-QPSK implementation

It is interesting to note that for baseband pulse functions satisfying

$$\eta p(d + mT) = \delta_m \tag{9}$$

for some fixed delay d and scale factor η (compare to the Nyquist criterion of Eq. (3)), $m(d + kT) = \pm jm(d + (k - 1)T)$, i.e., the OQPSK signal undergoes a net phase change of exactly 90° in each bit interval. The subset of OQPSK discussed in the next section will satisfy this condition.

MSK-Like Formats

What considerations are involved in creating a constant-envelope OQPSK signal, that is, in making $|m(t)|^2 = 1$ in Eq. (6) using a real baseband pulse function $p(t)$? Answering this question requires looking at the properties of $|m(t)|^2$. Take $m(t)$ as given by Eq. (6) and multiply by its conjugate:

$$|m(t)|^2 = m(t)\, m^*(t) = \sum_m \sum_n \beta_m \beta_n j^{m-n} p(t - mT)\, p(t - nT), \tag{10}$$

where the * superscript indicates complex conjugation. Since the $\{\beta_m\}$ are data-dependent, and thus unpredictable, the only way $|m(t)|^2$ can have a predictable value is if the only terms that contribute to

the double sum of Eq. (10) are those for which $m = n$. The resulting requirement is that $p(t - mT)\,p(t - nT) = 0$ for all t and $m \neq n$. With some simple substitution this becomes

$$p(t)\,p(t - mT) = 0; \quad m \neq 0,$$

which is easily seen to be equivalent to

$$p(t) = 0; \quad |t - t_0| > T \tag{11}$$

for some t_0, i.e., $p(t)$ can only be nonzero over an interval of $2T$ in t. Using this assumption that only terms for which $m = n$ can contribute to the sum of Eq. (10), Eq. (10) becomes

$$|m(t)|^2 = \sum_m p^2(t - mT). \tag{12}$$

Notice that this is periodic with period T. To force $|m(t)|^2$ to unity it will, therefore, be adequate to force it to unity over one period. Since Eq. (11) is assumed satisfied, only two terms of Eq. (12) contribute at any one time. Focusing in on one particular interval of width T,

$$|m(t)|^2 = p^2(t) + p^2(t + T); \quad t_0 - T \leqslant t < t_0. \tag{13}$$

Equating this to unity produces the second constant-envelope requirement,

$$p^2(t) + p^2(t + T) = 1; \quad t_0 - T \leqslant t < t_0. \tag{14}$$

Equations (11) and (14) are the two conditions that are frequently cited as defining the MSK-like subset of the OQPSK modulation formats (often with t_0 set to 0). The most well-known modulation format of this class is minimum-shift keying, or MSK, described by Eqs. (6) and (7) and

$$p(t) = \cos \frac{\pi t}{2T}; \quad |t| < T.$$

A close inspection of this definition reveals that MSK is also a special case of FSK (frequency-shift keying), with $s_c(t)$ of Eq. (1) having frequency $\omega_c + \pi/2T$ while a data 1 is being transmitted and frequency $\omega_c - \pi/2T$ while a data 0 is being transmitted. The "minimum" in minimum-shift keying refers to the tone spacing π/T, which is smaller than that used in most FSK systems.

There are two other well-known MSK-like modulation formats: SFSK (sinusoidal FSK) [2], described by

$$p(t) = \cos\left[\frac{\pi t}{2T} - \frac{1}{4}\sin\frac{2\pi t}{T}\right]; \quad |t| < T,$$

and DSFSK (doubly sinusoidal FSK) [3], described by

$$p(t) = \cos\left[\frac{\pi t}{2T} - \frac{1}{3}\sin\frac{2\pi t}{T} + \frac{1}{24}\sin\frac{4\pi t}{T}\right]; \quad |t| < T.$$

SFSK and DSFSK are not discussed further except for comparison of spectral rolloff properties with RSK below.

3. THE CLASS OF BASEBAND PULSE FUNCTIONS OPTIMIZED

Suppose an MSK-like modulation is desired using the implementation strategy outlined in Fig. 2. Further, suppose an implementation is desired with the Laplace transform of $f(t)$, denoted by $F(s)$, a rational function of s. (Throughout this report, upper and lowercase letters refer to the Laplace and time domains.) This would be necessary if the arm filters were to be implemented using conventional lumped-constant filter technology. Are there any obvious requirements on $F(s)$ that can be deduced from the constant-envelope conditions derived above?

Equation (11) requires that $p(t)$ be supported only over a finite interval. This implies that $P(s)$ can have no poles. Since $P(s) = G(s)F(s)$, $F(s)$ can have poles only where $G(s)$ has zeros (located at $s = \pm j k\pi/T$, $k = 1, 2 = \ldots$). The number of zeros of $F(s)$ can be determined by the desired spectral-rolloff properties of $P(s)$. Since there is no point to this exercise unless the spectrum of the resulting baseband pulse function rolls off faster than for rectangular QPSK, $F(s)$ should have at least one more pole than it has zeros. $F(s)$ can therefore be expressed as

$$F(s) = \sum_{k \geq 1} \frac{\sigma_k s + \rho_k}{s^2 + (k\pi/T)^2},$$

where the σ's and ρ's are real and only a finite number of terms have nonzero σ and ρ. Cascading this $F(s)$ with $G(s)$ effectively substitutes a (smaller) set of zeros in place of some (finite) set of the zeros of $G(s)$. The most obvious choice of a set of zeros to replace* is the set of $2n$ zeros in the region of the s-plane where $G(s)$ is generally the largest, i.e., near $s = 0$, effectively making the above sum range from $k = 1$ to $k = n$. The zeros of $F(s)$ can be further restricted by requiring $\sigma_k = 0$ in the expression above. Necessary for computational feasibility, this constrains the zeros of $F(s)$ to occur in pairs on the axes (real or imaginary) symmetric about the origin; this is convenient for certain popular realization strategies. The following results:

$$F(s) = \sum_{k=1}^{n} \frac{\rho_k}{s^2 + (k\pi/T)^2}. \tag{15}$$

The effect on $p(t)$ of this last restriction is to force it to be symmetric in time, i.e., $p(t_0 + t) = p(t_0 - t)$. It is worth noting that all of the well-known MSK-like modulation formats are symmetric in time.

The class of functions described by Eq. (15) can be described more conveniently for the purposes of this report as

$$F(s) = \frac{2\pi^2}{T^2} \sum_{k=1}^{n} \frac{k^2 a_k}{s^2 + (k\pi/T)^2}. \tag{16}$$

The additional constant factor and the change from ρ_k to $k^2 a_k$ will allow simpler expressions below.

Although the use of arm filters described by Eq. (16) in the OQPSK configuration of Fig. 2 results automatically in the satisfaction of the condition expressed in Eq. (11), it does not automatically result in the satisfaction of Eq (14). An optimization criterion will therefore be chosen in the following section that can be used to choose the coefficients $\{a_k\}$ in Eq. (16) so that either Eq. (14) *is* satisfied, or, more likely, Eq. (14) is *nearly* satisfied. There are two other constraints that need to be satisfied. One is the Nyquist criterion of Eq. (3), necessary to prevent intersymbol interference. The remaining constraint, necessary to ensure that the OQPSK signal experiences a net phase change of 90° in each bit interval, is given by Eq. (9). Notice that any function $p(t)$ satisfying Eq. (9) satisfies the Nyquist criterion of Eq. (3) automatically. For baseband pulse functions satisfying Eq. (11) the additional condition

$$p(t_0) \neq 0 \tag{17}$$

is sufficient (though not necessary) to ensure that Eq. (9) is satisfied. A reasonable strategy, therefore, is to perform the optimization first and then check to see whether Eq. (17) (or, if not Eq. (17), then Eq. (9)) is satisfied.

*Although it would be interesting to explore optimum arm-filter functions with zeros at various other combinations of the low-frequency zeros of $G(s)$, such a task is beyond the scope of this investigation.

It is convenient to express the optimization criterion in terms of $p(t)$. To find the baseband pulse function $p(t)$ implied by the transfer function of Eq. (16), the impulse response corresponding to Eq. (16) is first calculated by inverse Laplace transforming $F(s)$ (in a region of convergence $\mathrm{Re}\{s\} > 0$):

$$f(t) = \frac{2\pi}{T}\, U(t) \sum_{k=1}^{n} k a_k \sin \frac{k\pi t}{T}.$$

To obtain the pulse function $p(t)$, convolve $f(t)$ with the rectangular driving function $g(t)$. Because $f(t)$ is periodic with period $2T$ equal to the width of the gate function $g(t)$, the convolution will equal zero for $t \geqslant 2T$:

$$p(t) = \int_{-\infty}^{\infty} f(\tau)\, g(t-\tau)\, d\tau = g(t) \int_{0}^{t} f(\tau)\, d\tau,$$

or, performing the integration,

$$p(t) = g(t) \sum_{k=1}^{n} 2 a_k \left[1 - \cos \frac{k\pi t}{T}\right]. \tag{18}$$

It is interesting to note that if this pulse function were extended by letting the number of terms n in the sum approach infinity, it would become a Fourier series capable of representing any function that

(a) was real with finite-energy,

(b) had support only over the interval $0 < t < 2T$, and

(c) was symmetric with respect to $t = T$, i.e., $p(T + t) = p(T - t)$.

4. THE OPTIMIZATION CRITERION

The optimization criterion used to optimize the $\{a_k\}$ of Eq. (18) must be one which tends to represent the amplitude fluctuations in the OQPSK signal generated with the baseband pulse function of Eq. (18). To be able to deal with such quantities as "the average fluctuation" more precisely, it is helpful to reformulate the complex modulation function $m(i)$ of Eq. (6) as a random process. Let the transmitted data symbols β_m be independent random variables with the two possible values equiprobable, and interpret the summation over the index m as ranging from $m = -\infty$ to $m = \infty$. Make this random process stationary by inserting a random delay u, uniformly distributed from 0 to T. These changes produce

$$m_R(t) = \sum_{m} \beta_m j^m p(t - mT - u); \quad u \sim \mathrm{U}(0,T). \tag{19}$$

The subscript on the function $m_R(t)$ indicates a random process.

Given this formulation, one obvious strategy is to choose the $\{a_k\}$ of Eq. (18) to minimize the variance of $|m_R(t)|$ while holding the mean of $|m_R(t)|$ constant. Unfortunately, the mean of $|m_R(t)|$ is difficult to calculate. A slightly modified strategy proves easier: choose the $\{a_k\}$ of Eq. (18) to minimize the variance of $|m_R(t)|^2$ while holding the mean of $|m_R(t)|^2$ constant. The extra squaring has the added benefit of increasing the "penalty" associated with large envelope fluctuations. Appendix A shows that the mean of $|m_R(t)|^2$ is

$$E\{|m_R(t)|^2\} = 8\left\{\sum_{k=1}^{n} a_k\right\}^2 + 4\sum_{k=1}^{n} a_k^2, \tag{20}$$

and the variance of $|m_R(t)|^2$ is

$$\begin{aligned}\mathrm{Var}\{|m_R(t)|^2\} = \sum_{k=1}^{n}\sum_{i=1}^{n}\sum_{m=1}^{n}\sum_{r=1}^{n} a_k a_i a_m a_r \Big\{ & 2^7\, even(k)\, even(i)\, \delta_{k-i} \\ & - 2^4\, \delta_{k-i}\delta_{m-r} \\ & - 2^6\, even(k)\, (\delta_{k+i-m}+\delta_{k-i+m}+\delta_{k-i-m}) \\ & + 2^3\, even(k+i)\, (\ \delta_{k+i+m-r}+\delta_{k+i-m+r} \\ & \qquad +\delta_{k+i-m-r}+\delta_{k-i+m+r} \\ & \qquad +\delta_{k-i+m-r}+\delta_{k-i-m+r} \\ & \qquad +\delta_{k-i-m-r})\Big\}, \end{aligned} \tag{21}$$

where the function *even*( ) is defined to be unity if its integer argument is even and zero otherwise. Equations (20) and (21) will be evaluated separately below for the 4th-, 6th-, and 8th-order arm filters discussed in the next section.

Optimization Constraints to Control Spectral Rolloff

Since $F(s)$ in Eq. (16) has, in general, two more poles than zeros, its magnitude rolls off asymptotically with frequency at 12 dB/octave. Since $G(s)$ rolls off at 6 dB/octave, $P(s)$ rolls off at 18 dB/octave, faster than the 12 dB/octave of MSK but slower than the 24 dB/octave of SFSK. If faster spectral rolloff than 18 dB/octave is needed, the $\{a_k\}$ will have to be further constrained during optimization to force $F(s)$ to have fewer zeros.

To see what these constraints are, it is helpful to express the arm-filter transfer function $F(s)$ of Eq. (16) as a ratio. Giving $F(s)$ a common denominator produces

$$F(s) = \frac{2\pi^2}{T^2}\ \frac{\displaystyle\sum_{k=1}^{n} k^2 a_k \prod_{\substack{i=1 \\ i\neq k}}^{n} s^2 + (i\pi/T)^2}{\displaystyle\prod_{k=1}^{n} s^2 + (k\pi/T)^2}. \tag{22}$$

Before trying to put the numerator of this expression in the form of a single polynomial in s, consider expanding the simpler product,

$$\prod_{k=1}^{n}(s + b_k)\,.$$

This expands into a nth-degree polynomial in s, where the coefficient of s^{n-m} is

$$\sum_{\{i_1, i_2, \ldots, i_m\}\in\Psi_m^n} b_{i_1} b_{i_2} \cdots b_{i_m},$$

with Ψ_m^n defined to be the set of all combinations of m of the integers between 1 and n. When m is zero, Ψ_m^n is defined to contain only a single, empty combination. This makes the product of the $\{b_{i_k}\}$ empty, and thus equal to the identity element for multiplication: unity. Using this approach, the coefficient of $s^{2(n-m)}$ in the expansion of

$$\prod_{k=1}^{n} s^2 + (i\pi/T)^2$$

becomes

$$\sum_{\{i_1,i_2,\ldots,i_m\}\in\Psi_m^n} \frac{i_1^2\pi^2}{T^2}\,\frac{i_2^2\pi^2}{T^2}\cdots\frac{i_m^2\pi^2}{T^2}$$

or

$$\frac{\pi^{2m}}{T^{2m}} \sum_{\{i_1,i_2,\ldots,i_m\}\in\Psi_m^n} (i_1 i_2 \ldots i_m)^2 .$$

To modify this to take account of the $i \neq k$ condition in the product in the numerator of Eq. (22), replace the set of combinations Ψ_m^n with a modified set $\Theta_m^{n,k}$ defined to be the set of all combinations of m of the integers between 1 and n excluding k. The expression above will then give the coefficient of $s^{2(n-m-1)}$ in the expansion of the product. Again, $\Theta_0^{n,k}$ is the set containing only the empty combination. Equation (22) can now be rewritten as

$$F(s) = \frac{2\pi^2}{T^2}\,\frac{\displaystyle\sum_{m=0}^{n-1} s^{2(n-m-1)}\frac{\pi^{2m}}{T^{2m}} \sum_{k=1}^{n} k^2 a_k \sum_{\{i_1,i_2,\cdots,i_m\}\in\Theta_m^{n,k}} (i_1 i_2 \ldots i_m)^2}{\displaystyle\prod_{k=1}^{n} s^2 + (k\pi/T)^2}. \tag{23}$$

To obtain faster spectral rolloff of the baseband pulse function than 18 dB/octave requires constraining the $\{a_k\}$ in the optimization process so that the degree of the numerator of the arm-filter transfer function of Eq. (23) is reduced to less than $2n - 2$. To reduce the degree of the numerator by two to gain an additional 12 dB/octave requires setting the coefficient of the highest degree term in the numerator to zero,

$$\sum_{k=1}^{n} k^2 a_k = 0 . \tag{24}$$

Notice that the rightmost sum in Eq. (23) contained only an empty product. To reduce the degree of the numerator of Eq. (23) by four to gain 24 dB/octave requires Eq. (24) *and* setting the next coefficient to zero by requiring

$$\sum_{k=1}^{n} k^2 a_k \sum_{\substack{i=1 \\ i\neq k}}^{n} i^2 = 0 . \tag{25}$$

The only limit to the number of such constraints that can be applied is that at least one degree of freedom among the $\{a_k\}$ must remain for optimization.

5. THE RSK MODULATION FORMATS

The optimization of the $\{a_k\}$ of Eq. (16) (and Eq. (18)) according to the optimization criterion developed above is discussed separately below for 4th-, 6th-, and 8th-order arm filters. In each case, the following information is given:

- A name for each format, *RSK(m,n),* where m and n indicate the numbers of zero pairs and pole pairs in the rational transfer function.
- The optimum coefficients $\{a_k\}$ for use in Eqs. (16) and (18).
- A plot of the baseband pulse function $p(t)$ given in Eq. (18).

- A plot of one period of the magnitude of the complex-baseband OQPSK signal of Eq. (6). This is given by Eq. (13) with $t_0 = T$.

- The normalized zero locations $\{z_k\}$ and gain γ for the following factored equivalent of Eq. (16):

$$F(s) = \gamma \frac{\prod_{k=1}^{m} \left(\frac{Ts}{z_k} \right)^2 + 1}{\prod_{k=1}^{n} \left(\frac{Ts}{k\pi} \right)^2 + 1} . \tag{26}$$

- A plot of the spectral density of the OQPSK process of Eq. (19), shown in Appendix B to be

$$S_{m_R m_R^*}(\Omega_T) = 4\gamma^2 \frac{\sin^2 \Omega_T}{\Omega_T^2} \frac{\prod_{k=1}^{m} \left[1 - \left(\frac{\Omega_T}{z_k} \right)^2 \right]^2}{\prod_{k=1}^{n} \left[1 - \left(\frac{\Omega_T}{k\pi} \right)^2 \right]^2} . \tag{27}$$

  The spectral densities are shown in a form in which the spectral level is given as a function of a dimensionless frequency variable $\Omega_T = \Omega T$. This has the effect of making the density dimensionless as well.*

All of the above items except the plots are repeated in tabular form in the Summary.

Fourth-Order Arm Filters

Fourth-order arm filters are obtained by setting $n = 2$ in Eqs. (16) and (18). Evaluating Eq. (20) with $n = 2$ yields the mean squared amplitude

$$E\{|m_R(t)|^2\} = 12a_2^2 + 16a_1a_2 + 12a_1^2. \tag{28}$$

Similarly, evaluating Eq. (21) with $n = 2$ yields the variance of the squared amplitude

$$\mathrm{Var}\{|m_R(t)|^2\} = 136a_2^4 + 256a_1a_2^3 + 64a_1^2a_2^2 - 64a_1^3a_2 + 8a_1^4. \tag{29}$$

The optimization problem can be formulated using a Lagrange multiplier. Define the Lagrangian

$$L = \mathrm{Var}\{|m_R(t)|^2\} - \mu\,(E\{|m_R(t)|^2\} - 1) \tag{30}$$

or, substituting from Eqs. (29) and (28),

$$\begin{aligned} L = {} & 136a_2^4 + 256a_1a_2^3 + 64a_1^2a_2^2 - 64a_1^3a_2 + 8a_1^4 \\ & + \mu\,(12a_2^2 + 16a_1a_2 + 12a_1^2 - 1)\,. \end{aligned}$$

The variable μ is a Lagrange multiplier introduced to force the factor that it multiplies to equal zero in the optimization solution. The optimization now proceeds by setting the gradient of the Lagrangian (with respect to the three variables a_1, a_2, and μ) to zero and solving for the stationary points of the Lagrangian. Computing the gradient and equating to zero produces

$$\begin{aligned} 0 &= 256a_2^3 + 128a_1a_2^2 - 192a_1^2a_2 + 32a_1^3 + \mu(16a_2 + 24a_1) \\ 0 &= 544a_2^3 + 768a_1a_2^2 + 128a_1^2a_2 - 64a_1^3 + \mu(24a_2 + 16a_1) \\ 0 &= 12a_2^2 + 16a_1a_2 + 12a_1^2 - 1\,. \end{aligned}$$

*Of course, if the pulse function were to be given units, the corresponding normalized spectral densities would have units as well. For example, if $p(t)$ were expressed in volts, the corresponding normalized spectral density would have units of volts^2.

Solving this set of simultaneous equations numerically produced the stationary points given in Table 1. The negative of each solution shown is also a stationary point (of the same type and with the same variance) due to the symmetry of the problem. As the choice of the sign of $p(t)$ is irrelevant in most practical applications, only one of each such pair of solutions is given.

Table 1 — Lagrangian Stationary Points with $n = 2$

a_1	a_2	$\mathrm{Var}\{\lvert m_R(t)\rvert^2\}$
0.25143	0.05195	5.85147×10^{-5}
0.31903	−0.37636	0.16243
0.38542	−0.22858	0.70375
0.05863	−0.32443	1.02166

A discriminant test on the constraint equation

$$12a_2^2 + 16a_1a_2 + 12a_1^2 = 1$$

shows that it describes an ellipse in the (a_1, a_2) plane. Since it describes a closed line, the global minimum of the variance on that line is just the stationary point for which the variance is smallest, i.e.,

$$a_1 = 0.25143, \quad a_2 = 0.05195.$$

The baseband pulse function obtained by substituting these values into Eq. (18) with $n = 2$ is plotted in Fig. 3. Since it is nonzero in the center as required by Eq. (17), it satisfies the 90° net-phase-change criterion of Eq. (9) and the Nyquist (zero-intersymbol-interference) criterion of Eq. (3) automatically. Figure 4 shows the $i(t)$ and $q(t)$ waveforms of Fig. 2 that would result from using the arm filters that correspond to this baseband pulse function.

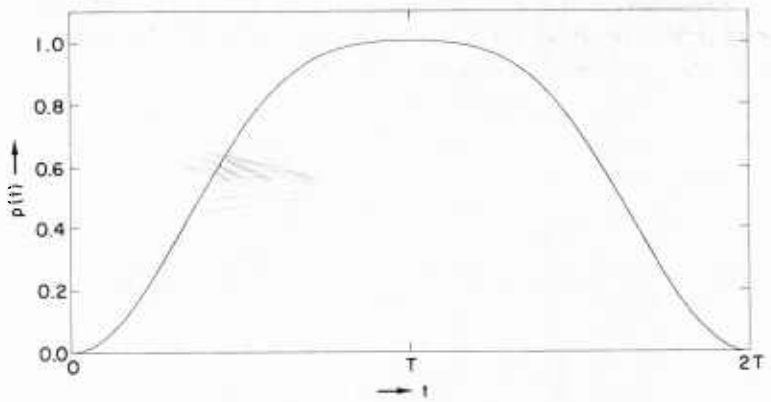

Fig. 3 — Baseband pulse function from optimum fourth-order arm filter

Figure 5 shows one period of the magnitude (calculated using Eq. (13)) of the complex-baseband OQPSK signal of Eq. (6) using the baseband pulse function of Fig. 3. This shows that the square root of the sum of the squares of the i and q waveforms of Fig. 4 would fluctuate less than 1% from its mean. The amplitude variations are so small as to be practically negligible.

If the transfer function of the arm filter is put into the factored form of Eq. (26), there is one pair of imaginary zeros ($m = 1$) and the gain constant and zero location are given by

$$\gamma = 0.606768, \quad z_1 = 1.62557\,\pi.$$

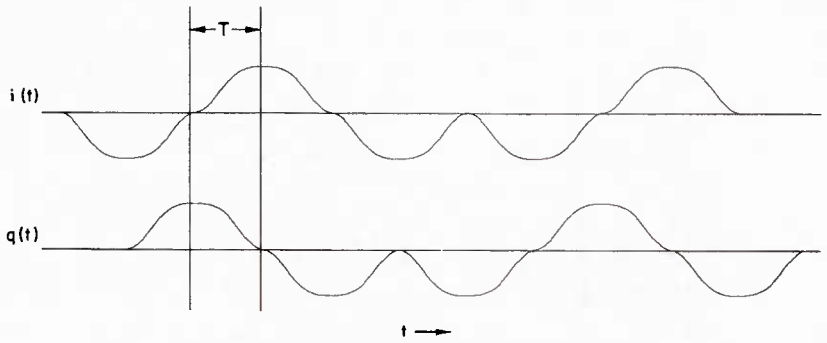

Fig. 4 — Typical i and q waveforms using the fourth-order arm filters

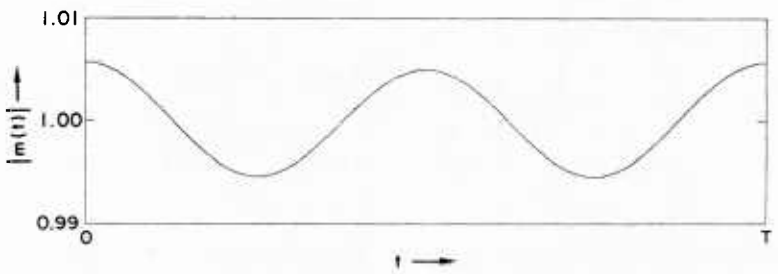

Fig. 5 — One period of the envelope of the fourth-order RSK signal

The spectral density of the fourth-order RSK process is shown in Fig. 6 along with the spectral density of the MSK and SFSK processes, for comparison. All three densities are normalized to unit total power. The RSK density appears to be between the MSK and SFSK densities in several ways: spectral density at zero frequency, width of main spectral lobe, height of first sidelobe, and asymptotic rolloff rate. Thus, the fourth-order RSK modulation format can be used where a compromise between the spectral properties of MSK and SFSK is needed.

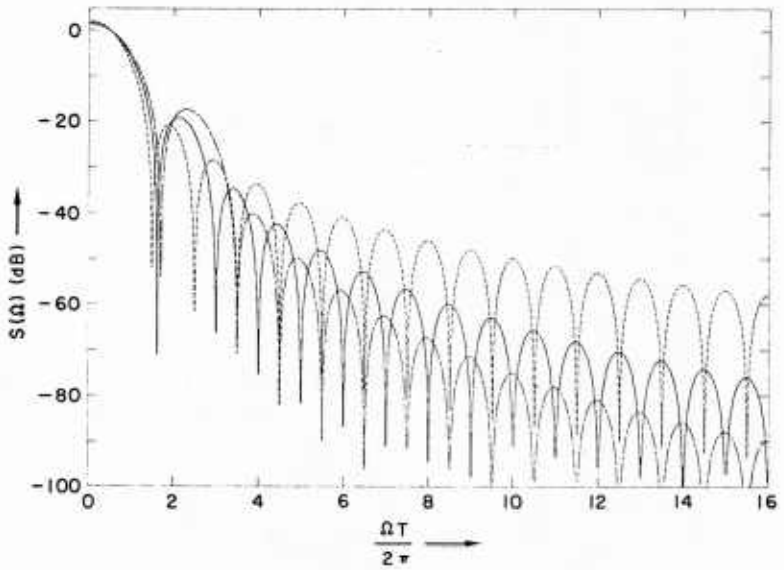

Fig. 6 — Spectral densities of fourth-order RSK (solid), MSK (dashed), and SFSK (chain-dashed)

Sixth-Order Arm Filters

Sixth-order arm filters are obtained by setting $n = 3$ in Eqs. (16) and (18). Evaluating Eq. (20) with $n = 3$ yields the mean squared amplitude

$$E\{|m_R(t)|^2\} = 12a_3^2 + 4a_1(4a_3 + 4a_2) + 16a_2a_3 + 12a_2^2 + 12a_1^2.$$

Similarly, evaluating Eq. (21) with $n = 3$ yields the variance of the squared amplitude

$$\begin{aligned}\mathrm{Var}\{|m_R(t)|^2\} = {} & 8a_3^4 + 128a_2^2a_3^2 - 128a_1a_2a_3^2 + 64a_1^2a_3^2 + 256a_2^3a_3 + 160a_1a_2^2a_3 \\ & - 192a_1^2a_2a_3 + 32a_1^3a_3 + 136a_2^4 + 256a_1a_2^3 + 64a_1^2a_2^2 - 64a_1^3a_2 + 8a_1^4.\end{aligned}$$

The optimization of this variance with only a mean-squared amplitude constraint would lead to a pulse $p(t)$ with an asymptotic spectral rolloff rate no better than that associated with the fourth-order problem solved earlier. The extra degree of freedom inherent in the sixth-order problem would be expected to lead to a solution with lower variance, but, since the variance obtained by the simpler fourth-order solution is adequate for any practical application, there is little point in looking for a higher order filter function with the same rolloff rate. To obtain a higher rolloff rate, the constraint given by Eq. (24) can be used to force the sixth-order transfer function $F(s)$ to have four more poles than zeros. Solving Eq. (24) (with $n = 3$) for a_1 gives

$$a_1 = -9a_3 - 4a_2.$$

Substitution of this expression for a_1 into the expressions just given for the mean and variance of the squared amplitude gives the constrained mean

$$E\{|m_R(t)|^2\} = 840a_3^2 + 672a_2a_3 + 140a_2^2,$$

and the constrained variance

$$\mathrm{Var}\{|m_R(t)|^2\} = 34352a_3^4 + 99072a_2a_3^3 + 102176a_2^2a_3^2 + 42880a_2^3a_3 + 6280a_2^4.$$

The optimization problem can now be formulated using a Lagrange multiplier. The use of the Lagrangian form given in Eq. (30) with the constrained mean and variance above gives

$$\begin{aligned}L = {} & 34352a_3^4 + 99072a_2a_3^3 + 102176a_2^2a_3^2 + 42880a_2^3a_3 + 6280a_2^4 \\ & + \mu(840a_3^2 + 672a_2a_3 + 140a_2^2 - 1).\end{aligned}$$

Computing the gradient of this Lagrangian and equating it to zero produces three simultaneous nonlinear equations in three unknowns:

$$\begin{aligned}0 = {} & 99072a_3^3 + 204352a_2a_3^2 + 128640a_2^2a_3 + 25120a_2^3 \\ & + \mu(672a_3 + 280a_2)\end{aligned}$$

$$\begin{aligned}0 = {} & 137408a_3^3 + 297216a_2a_3^2 + 204352a_2^2a_3 + 42880a_2^3 \\ & + \mu(1680a_3 + 672a_2)\end{aligned}$$

$$0 = 840a_3^2 + 672a_2a_3 + 140a_2^2 - 1.$$

Solving this set of simultaneous equations numerically produced the stationary points given in Table 2. Again, due to the symmetry inherent in the problem, the negative of each solution shown is also a stationary point.

Table 2 — Lagrangian Stationary Points with $n = 3$ and a_1 Constrained

a_1	a_2	a_3	Var $\{\|m_R(t)\|^2\}$
0.29031	0.04595	−0.05268	6.56782×10^{-3}
−0.18456	0.42203	−0.16706	0.47046
0.04338	0.34356	−0.15751	0.94788
0.34040	−0.29482	0.09321	1.12266

A discriminant test on the constraint equation

$$840a_3^2 + 672a_2a_3 + 140a_2^2 = 1$$

shows that it describes an ellipse in the (a_2, a_3) plane. Since it describes a closed line, the global minimum of the variance on that line is just the stationary point for which the variance is smallest, i.e.,

$$a_1 = 0.29031, \quad a_2 = 0.04595, \quad a_3 = -0.05268.$$

The baseband pulse function obtained by substituting these values into Eq. (18) with $n = 3$ is plotted in Fig. 7. Since it is nonzero in the center as required by Eq. (17), it satisfies the 90° net-phase-change criterion of Eq. (9) and the Nyquist (zero-intersymbol-interference) criterion of Eq. (3) automatically.

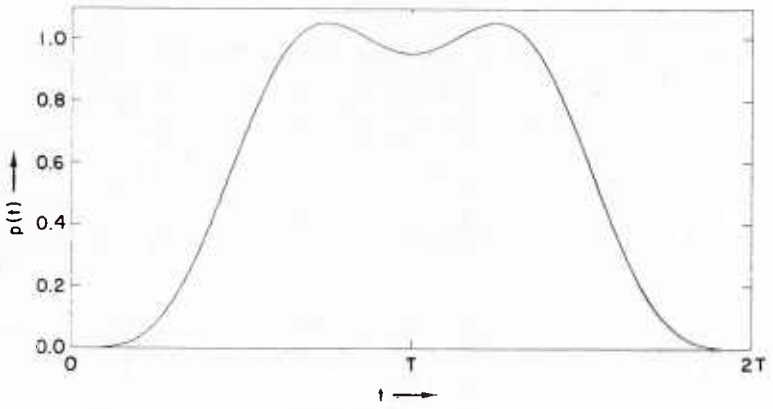

Fig. 7 — Baseband pulse function from optimum sixth-order arm filter

The pronounced dip in the middle of the pulse function shown in Fig. 7 is consistent with the relativley large (squared-amplitude) variance implied by Table 2. This effect is shown more clearly in Fig. 8, which shows one period of the magnitude (calculated using Eq. (13)) of the complex-baseband OQPSK signal of Eq. (6) using the baseband pulse function of Fig. 7. While this high envelope ripple may be intolerable in some applications, it may be possible to tolerate it in others in order to obtain the associated spectral characteristics given in Fig. 9.

The spectral density of the sixth-order RSK process in Fig. 9 is shown along with the spectral density of the SFSK and DSFSK processes, for comparison. All three densities are normalized to unit total power. The RSK density appears to be between the SFSK and DSFSK densities in several ways: spectral density at zero frequency, width of main spectral lobe, height of first sidelobe, and asymptotic rolloff rate. The RSK spectrum is, however, clearly superior to the DSFSK spectrum for the first few sidelobes. Thus, while the DSFSK spectrum is generally thought so poor as to preclude the implementation of DSFSK, the RSK(2,6) format may be useful where a higher rolloff rate is needed than is provided by SFSK and where the substantial ripple of RSK(2,6) is tolerable.

If the transfer function of the arm filter is put into the form given by Eq. (26), there is one pair of imaginary zeros ($m = 1$) and the gain constant and zero location are given by

$$\gamma = 0.56716, \quad z_1 = 1.77465\pi.$$

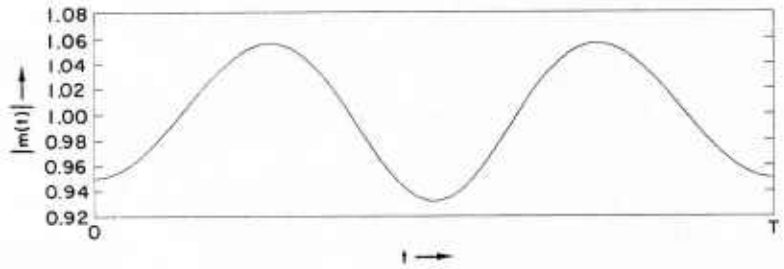

Fig. 8 — One period of the envelope of the sixth-order RSK signal

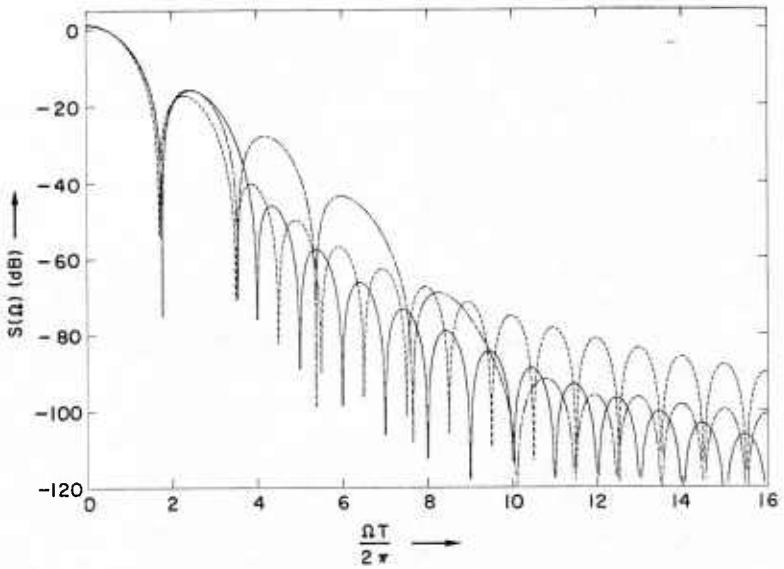

Fig. 9 — Spectral densities of sixth-order RSK (solid), SFSK (dashed), and DSFSK (chain-dashed)

Eighth-Order Arm Filters

To obtain the 30 dB/octave asymptotic spectral rolloff of the previous section without the associated envelope ripple requires adding another degree of freedom to the optimization by moving from a sixth-order arm filter to an eighth-order arm filter. Eighth-order arm filters are obtained by setting $n = 4$ in Eqs. (16) and (18). Evaluating Eq. (20) with $n = 4$ yields the mean squared amplitude

$$E\{|m_R(t)|^2\} = 12a_4^2 + 16a_3a_4 + 16a_2a_4 + 16a_1a_4 + 12a_3^2 + 16a_2a_3 + 16a_1a_3 + 12a_2^2 + 16a_1a_2 + 12a_1^2.$$

Similarly, evaluating Eq. (21) with $n = 4$ yields the variance of the squared amplitude

$$\begin{aligned}\mathrm{Var}\{|m_R(t)|^2\} = {} & 136a_4^4 + 256a_3a_4^3 + 256a_2a_4^3 + 256a_1a_4^3 + 128a_3^2a_4^2 + 256a_2a_3a_4^2 \\ & + 128a_1a_3a_4^2 + 128a_2^2a_4^2 + 256a_1a_2a_4^2 + 128a_1^2a_4^2 + 32a_2a_3^2a_4 \\ & - 128a_1a_3^2a_4 + 64a_2^2a_3a_4 - 192a_1a_2a_3a_4 - 128a_1^2a_3a_4 + 64a_2^3a_4 \\ & + 64a_1a_2^2a_4 - 32a_1^2a_2a_4 + 8a_3^4 + 128a_2^2a_3^2 - 128a_1a_2a_3^2 + 64a_1^2a_3^2 \\ & + 256a_2^3a_3 + 160a_1a_2^2a_3 - 192a_1^2a_2a_3 + 32a_1^3a_3 + 136a_2^4 + 256a_1a_2^3 \\ & + 64a_1^2a_2^2 - 64a_1^3a_2 + 8a_1^4.\end{aligned}$$

The optimization of this variance with only a mean-squared amplitude constraint would lead to a pulse $p(t)$ with an asymptotic spectral rolloff rate no better than that associated with the fourth-order problem solved earlier. To obtain a higher rolloff rate, the constraint given by Eq. (24) can be used to force the eighth-order transfer function $F(s)$ to have four more poles than zeros. Solving Eq. (24) (with $n=4$) for a_1 gives

$$a_1 = -16a_4 - 9a_3 - 4a_2.$$

Substitution of this expression for a_1 into the expressions just given for the mean and variance of the squared amplitude gives the constrained mean

$$E\{|m_R(t)|^2\} = 2828a_4^2 + 3072a_3a_4 + 1232a_2a_4 + 840a_3^2 + 672a_2a_3 + 140a_2^2$$

and the constrained variance

$$\begin{aligned}\mathrm{Var}\{|m_R(t)|^2\} = {} & 553096a_4^4 + 1048576a_3a_4^3 + 789760a_2a_4^3 + 765056a_3^2a_4^2 \\ & + 1163776a_2a_3a_4^2 + 405632a_2^2a_4^2 + 258048a_3^3a_4 + 581312a_2a_3^2a_4 \\ & + 404992a_2^2a_3a_4 + 85312a_2^3a_4 + 34352a_3^4 + 99072a_2a_3^3 + 102176a_2^2a_3^2 \\ & + 42880a_2^3a_3 + 6280a_2^4.\end{aligned}$$

In theory, the optimization problem can now be formulated using a Lagrange multiplier as was done earlier when solving for the fourth- and sixth-order arm filters. In practice, however, the resulting set of four simultaneous nonlinear equations in four unknowns proved too difficult to solve using the computational facilities at hand.

As an alternative, an iterative search program was used to search the (a_2, a_3) space for a minimum of the constrained variance expression above. For each (a_2, a_3) point, a_4 was calculated by evaluating the constrained mean (given above) at the (a_2, a_3) point in question, setting the resulting expression to unity, and solving the resulting quadratic equation in a_4. Each point in (a_2, a_3) space thus provided two points in (a_2, a_3, a_4) space at which to evaluate the constrained variance.

From a starting point at which a_2 and a_3 were equal to the values given earlier as the optimums for the sixth-order arm filter, the search rapidly converged on a minimum, shown in Table 3. The corresponding variance was 1.25202×10^{-6}, smaller even than the fourth order optimum. This is not surprising, in view of the extra degree of freedom here.

Table 3 — Minimum-Variance Point with $n=4$ and a_1 Constrained

k	a_k
1	0.28130
2	0.05200
3	−0.03141
4	−0.01291

Due to the nature of the method employed to find this minimum, there is no way to be certain it is a global minimum. This is not important, however, because this solution does have the properties desired. The baseband pulse function $p(t)$ obtained by substituting the values of Table 3 into Eq. (18) with $n = 4$ is plotted in Fig. 10. Once again, since it is nonzero in the center as required by Eq. (17), it satisfies the 90° net-phase-change criterion of Eq. (9) and the Nyquist (zero-intersymbol-interference) criterion of Eq. (3) automatically.

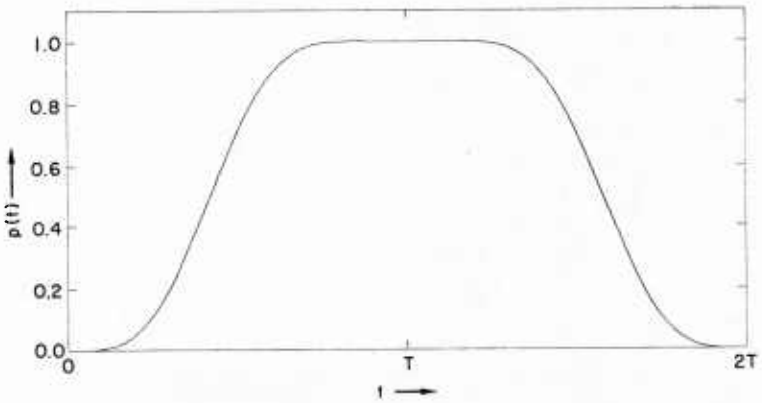

Fig. 10 — Baseband pulse function from optimum eighth-order arm filter

Figure 11 shows one period of the magnitude (calculated using Eq. (13)) of the complex-baseband OQPSK signal of Eq. (6) using the baseband pulse function of Fig. 10. The amplitude variations are even smaller than those shown in Fig. 5 for the fourth-order case.

If the transfer function of the arm filter is put into the form given by Eq. (26), there are two pairs of imaginary zeros ($m = 2$) and the gain constant and zero locations are given by

$$\gamma = 0.57795, \quad z_1 = 1.72733\,\pi, \quad \text{and} \quad z_2 = 3.43183\,\pi.$$

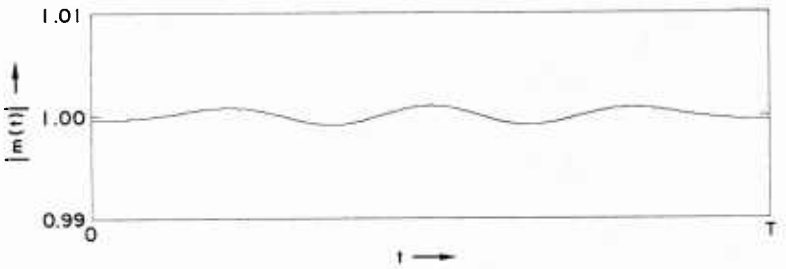

Fig. 11 — One period of the envelope of the eighth-order RSK signal

The spectral density of the eighth-order RSK process is shown in Fig. 12 along with the spectral density of the SFSK and DSFSK processes, for comparison. All three densities are normalized to unit total power. Like the sixth-order RSK spectrum shown in Fig. 9, the eighth-order RSK spectrum appears to be between the SFSK and DSFSK densities in several ways: spectral density at zero frequency, width of main spectral lobe, height of first sidelobe, and asymptotic rolloff rate. The RSK spectrum is, however, clearly superior to the DSFSK spectrum for the first few sidelobes. Figure 13 illustrates the tradeoff between the sixth- and eighth-order RSK formats by showing their spectra together for comparison. Clearly, the more constant envelope attained in the eighth-order case was at the expense of desired spectral qualities. The eighth-order RSK spectrum has a substantially higher second sidelobe, as well as somewhat higher sidelobes in the high-frequency rolloff region. The eighth-order RSK format is therefore preferred over the sixth-order format only when the much lower envelope ripple justifies both the added complexity and a somewhat poorer spectrum.

6. SUMMARY

Three new baseband pulse functions were derived for OQPSK signalling. I describe them as "almost MSK-like" because the OQPSK signals generated using these pulse functions (a) change phase

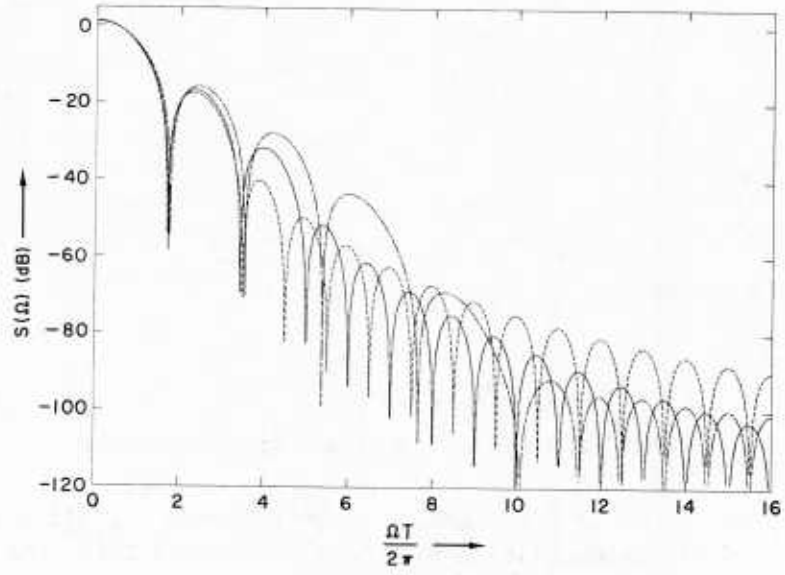

Fig. 12 — Spectral densities of eighth-order RSK (solid), SFSK (dashed), and DSFSK (chain-dashed)

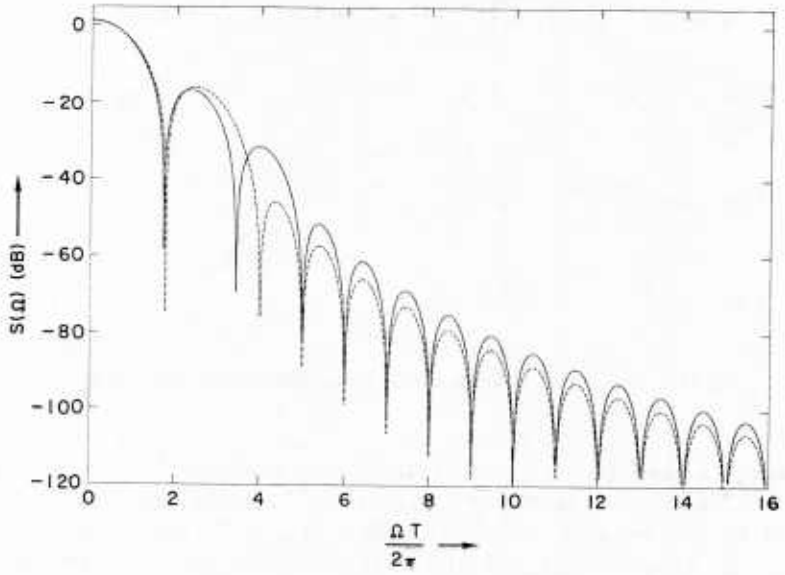

Fig. 13 — Spectral densities of sixth-order RSK (solid) and eighth-order RSK (dashed)

by exactly 90° in a bit interval and (b) have almost constant amplitude. In addition, the new formats have asymptotic spectral rolloff rates greater than the 12 dB/octave of MSK. These properties in OQPSK modulation types generally result in robust waveforms better able to tolerate the nonlinearities in high-power traveling-wave tube (TWT) amplifiers than conventional modulation types. Thus, these new modulation formats should prove especially useful where TWT operation at saturation is desired (and the wider central spectral lobe can be tolerated), such as in pulse-compression radar systems and in certain satellite data-communication systems.

The mathematical form of the new pulse functions is a sum of raised cosines:

$$p(t) = \begin{cases} \sum_{k=1}^{n} 2a_k \left[1 - \cos \frac{k\pi t}{T}\right], & 0 < t < 2T ; \\ 0 \text{ elsewhere.} \end{cases}$$

The form itself suggests implementation of these formats by physical generation of the raised-cosine waveforms for summing into two trains (in-phase and quadrature baseband components) of shaped pulses that can be polarity-switched by the data streams. This is similar to a commonly used strategy for generating MSK.

Another method of generating these modulation formats is suggested (from Eqs. (5), (8), and (26) and Fig. 2) by writing the Laplace transform of the baseband pulse function $p(t)$ in the following form:

$$F(s) = \frac{(1 - e^{-s2T})}{s} \cdot \frac{\gamma \prod_{k=1}^{m} \left(\frac{Ts}{z_k}\right)^2 + 1}{\prod_{k=1}^{n} \left(\frac{Ts}{k\pi}\right)^2 + 1} .$$

This is the Laplace transform of the rectangular pulse function (of rectangular OQPSK) multiplied by a rational transfer function. This transfer function can be approximately implemented (putting the poles as close to the imaginary axis as possible) in simple arm filters and used to shape NRZ data waveforms in the i and q channels. I have called these new modulation formats *rational-shift keying*, emphasizing both the similarity to MSK and the rational transfer functions in the Laplace transform of the pulse formats. Each format is denoted by *RSK(m,n)*, where m and n indicate the numbers of zero pairs and pole pairs in the rational transfer function.

The parameters n, a_k, γ, m, and z_k in the above equations are shown in Table 4 and were chosen (for each combination of m and n) to minimize the variance of the amplitude squared of a unit-power baseband OQPSK random process. Along with the RSK parameters, Table 4 gives this associated variance, the peak-to-peak amplitude ripple, the amount the first spectral sidelobe is down from the peak, and the asymptotic spectral rolloff rate.

Table 4 — Summary of RSK Parameters and Characteristics

Parameter	RSK(2,4)	RSK(2,6)	RSK(4,8)
a_1	0.25143	0.29031	0.28130
a_2	0.05195	0.04595	0.05200
a_3		−0.05268	−0.03141
a_4			−0.01291
γ	0.606768	0.56716	0.57795
z_1	1.62557π	1.77465π	1.72733π
z_2			3.43183π
Var $\{\lvert m_R(t)\rvert^2\}$	5.85147×10^{-5}	6.56782×10^{-3}	1.25202×10^{-6}
Peak-to-peak envelope fluctuation	0.0111	0.1237	0.0019
Spectral rolloff rate	18 dB/octave	30 dB/octave	30 dB/octave
Peak-to-first-sidelobe ratio	21.0 dB	17.12 dB	18.04 dB
OQPSK spectral density	Figure 6	Figure 9	Figure 12
Baseband pulse function	Figure 3	Figure 7	Figure 10
Envelope	Figure 5	Figure 8	Figure 11

7. REFERENCES

1. S. Pasupathy, "Minimum Shift Keying: A Spectrally Efficient Modulation," *IEEE Commun. Mag.* **17**(4), 14-22 (July 1979).

2. F. Amoroso, "Pulse and Spectrum Manipulation in the Minimum (Frequency) Shift Keying (MSK) Format," *IEEE Trans. Commun.* **COM-24**(3), 381-384 (March 1976).

3. B. Bazin, "A Class of MSK Baseband Pulse Formats with Sharp Spectral Roll-Off," *IEEE Trans. Commun.* **COM-27**(5), 826-829 (May 1979).

Appendix A
THE MEAN AND VARIANCE OF THE SQUARED AMPLITUDE

In this appendix, I calculate the mean and variance of the squared amplitude of the OQPSK process described by Eqs. (18) and (19). I calculate the variance by calculating the second and fourth moments of the amplitude of the process and then using

$$\mathrm{Var}\{|m_R(t)|^2\} = E\{|m_R(t)|^4\} - (E\{|m_R(t)|^2\})^2, \tag{A1}$$

to obtain the variance from those second and fourth moments.

The Fourth Moment of the Amplitude

I first calculate the fourth moment of the amplitude of the OQPSK process described by Eq. (19) with no restrictions* on the real baseband pulse function $p(t)$. The $p(t)$ of Eq. (18) is considered later as a special case of the general result.

The General Result: Real Baseband Pulse Functions

The integration over the uniform random variable u in Eq. (19) is made explicit when the desired moment is formulated in terms of a conditional expectation:

$$E\{|m_R(t)|^4\} = \frac{1}{T}\int_0^T E\{|m_R(t)|^4 \Big| u\}\, du\,. \tag{A2}$$

Now, calculate that conditional expectation by substituting for $m_R(t)$ from Eq. (19) and factoring all the nonrandom variables (including u, in this context) out of the expectation:

$$E\{|m_R(t)|^4 \Big| u\} = \sum_i \sum_k \sum_m \sum_n [E\{\beta_i\beta_k\beta_m\beta_n\}\, j^i\, j^k\, j^{-m}\, j^{-n} \cdot p(t - iT - u)\, p(t - kT - u)\, p(t - mT - u)\, p(t - nT - u)]. \tag{A3}$$

The baseband pulse function $p(t)$ has been assumed real. Consider the remaining expectation $E\{\beta_i\beta_k\beta_m\beta_n\}$. Because the expectation of a product of independent random variables is equal to the product of the expectations of those variables, and because the expectations of each of the $\{\beta_k\}$ is zero, $E\{\beta_i\beta_k\beta_m\beta_n\}$ will be zero whenever at least one of the indices i, k, m, and n is *different* from all of the others. In the complementary case in which each index is *equal* to at least one of the others, each β appearing in the product appears twice, removing the sign information. Therefore, using symbols $\wedge$ for logical conjunction ("and") and $\vee$ for logical disjunction ("or"),

$$E\{\beta_i\beta_k\beta_m\beta_n\} = \begin{cases} & \vee\ i=k \wedge m=n\,, \\ 1 & \vee\ i=m \wedge k=n\,, \\ & \vee\ i=n \wedge k=m\,; \\ 0 & \text{otherwise}\,. \end{cases}$$

*Other than those necessary to assure the convergence of various sums and integrals; convergence is not discussed explicitly but is assured for $p(t)$ of practical interest.

Noting that the three cases where the expectation equals unity overlap only where the four indices are all equal, the quadruple sum of Eq. (A3) can be written as a single sum for the case where the indices are all equal plus three double sums for the three cases where the indices are equal in pairs:

$$\begin{aligned} E\{|m_R(t)|^4 \big| u\} = & \sum_k p^4(t - kT - u) \\ & + \sum_k \sum_{m \neq k} (-1)^{k-m} p^2(t - kT - u)\, p^2(t - mT - u) \\ & + \sum_i \sum_{n \neq i} p^2(t - iT - u)\, p^2(t - nT - u) \\ & + \sum_i \sum_{m \neq i} p^2(t - iT - u)\, p^2(t - mT - u). \end{aligned}$$

Changing some indices and combining the last three sums produce the more compact

$$E\{|m_R(t)|^4 \big| u\} = \sum_k p^4(t - kT - u) + \sum_k \sum_{m \neq k} [2 + (-1)^{k-m}]\, p^2(t - kT - u)\, p^2(t - mT - u).$$

This can now be substituted back into Eq. (A2) and the integration brought inside the summations over k.

$$\begin{aligned} E\{|m_R(t)|^4\} = & \frac{1}{T} \sum_k \int_0^T p^4(t - kT - u)\, du \\ & + \frac{1}{T} \sum_k \int_0^T \sum_{m \neq k} [2 + (-1)^{k-m}]\, p^2(t - kT - u)\, p^2(t - mT - u)\, du. \end{aligned}$$

Applying the change of variables $\tau = t - kT - u$ in both integrals gives

$$\begin{aligned} E\{|m_R(t)|^4\} = & \frac{1}{T} \sum_k \int_{t-(k+1)T}^{t-kT} p^4(\tau)\, d\tau \\ & + \frac{1}{T} \sum_k \int_{t-(k+1)T}^{t-kT} \sum_{m \neq k} [2 + (-1)^{k-m}]\, p^2(\tau)\, p^2(\tau + (k - m)T)\, d\tau. \end{aligned}$$

It is now clear that the sums over k can be eliminated in favor of infinite limits on the integrals. Changing the index in the remaining sum to $n = k - m$ simplifies the equation further:

$$E\{|m_R(t)|^4\} = \frac{1}{T} \int_{-\infty}^{\infty} p^4(\tau)\, d\tau + \frac{1}{T} \int_{-\infty}^{\infty} \sum_{n \neq 0} [2 + (-1)^n]\, p^2(\tau)\, p^2(\tau + nT)\, d\tau.$$

Finally, the expression can be compacted by combining the integrals into one and expressing the first term as the missing $n = 0$ term of the sum, using a Kronecker delta function to get the coefficient right.

$$E\{|m_R(t)|^4\} = \frac{1}{T} \int_{-\infty}^{\infty} \sum_n [2(1 - \delta_n) + (-1)^n]\, p^2(\tau)\, p^2(\tau + nT)\, d\tau. \tag{A4}$$

Equation (A4) is the general expression for the fourth moment of the amplitude of this OQPSK process for real baseband pulse functions.

Special Case: Baseband Pulse Functions With Limited Support

Now, consider the special case of baseband pulse functions (such as those of Eq. (18)) satisfying the finite support restriction

$$p(t) = 0; \quad |t - T| \geq T. \tag{A5}$$

For this class of $p(t)$ the product $p^2(\tau)\, p^2(\tau + nT)$ is zero for all $n \geq 2$. The sum in Eq. (A4) therefore has at most three nonzero terms. Writing these out explicitly, distributing the integration over the sum, and shrinking the limits of integration to the smallest regions that might be nonzero produces

$$E\{|m_R(t)|^4\} = \frac{1}{T}\int_0^{2T} p^4(\tau)\,d\tau + \frac{1}{T}\int_0^{T} p^2(\tau)\,p^2(\tau+T)\,d\tau + \frac{1}{T}\int_T^{2T} p^2(\tau)\,p^2(\tau-T)\,d\tau.$$

A change of variable, $t = \tau - T$, in the integral third integral makes it identical to the second. Carrying out this change and splitting the first integral into two, one from 0 to T and one from T to $2T$, gives

$$E\{|m_R(t)|^4\} = \frac{1}{T}\int_0^{T} p^4(\tau)\,d\tau + \frac{1}{T}\int_T^{2T} p^4(\tau)\,d\tau + \frac{2}{T}\int_0^{T} p^2(\tau)\,p^2(\tau+T)\,d\tau.$$

Changing variables in the second integral by letting $t = \tau - T$ gives all three integrals the same limits and allows them to be combined into a single integral with the integrand a perfect square;

$$E\{|m_R(t)|^4\} = \frac{1}{T}\int_0^{T} [p^2(\tau) + p^2(\tau+T)]^2\,d\tau, \tag{A6}$$

which is the desired result for $p(t)$ satisfying Eq. (A5).

More Special Case: Baseband Pulse Functions as Sums of Raised Cosines

I now evaluate the fourth moment given by Eq. (A6) for baseband pulse functions described by Eq. (18). I begin by using Eq. (18) to build up the integrand of Eq. (A6), simplifying where possible. From Eq. (18) the square of the baseband pulse function can be written

$$p^2(t) = g(t)\sum_{k=1}^{n}\sum_{i=1}^{n} 2^2 a_k a_i \left[1 - \cos\frac{k\pi t}{T}\right]\left[1 - \cos\frac{i\pi t}{T}\right]. \tag{A7}$$

Also needed in the integrand of Eq. (A6) is this same quantity advanced by time T:

$$p^2(t+T) = g(t+T)\sum_{k=1}^{n}\sum_{i=1}^{n} 2^2 a_k a_i \left[1 - \cos\frac{k\pi(t+T)}{T}\right]\left[1 - \cos\frac{i\pi(t+T)}{T}\right].$$

Since $\cos(\phi + k\pi) = (-1)^k\cos(\phi)$, this can be rewritten

$$p^2(t+T) = g(t+T)\sum_{k=1}^{n}\sum_{i=1}^{n} 2^2 a_k a_i \left[1 - (-1)^k\cos\frac{k\pi t}{T}\right]\left[1 - (-1)^i\cos\frac{i\pi t}{T}\right].$$

This can now be summed with Eq. (A7) and the raised-cosine products multiplied out to give

$$p^2(t) + p^2(t+T) = \sum_{k=1}^{n}\sum_{i=1}^{n} 2^2 a_k a_i \left\{2 - [1 + (-1)^k]\cos\frac{k\pi t}{T} - [1 + (-1)^i]\cos\frac{i\pi t}{T} + [1 + (-1)^{k+i}]\cos\frac{k\pi t}{T}\cos\frac{i\pi t}{T}\right\}, \tag{A8}$$

where the product of the gate functions, not shown here, limits the validity of this equation to the range $0 \leqslant t < T$. Because this interval is compatible with the limits of integration in Eq. (A6), the gating functions will not be shown explicitly in the remainder of the derivation.

Notice that the second term in the large summand factor in Eq. (A8) differs from the third term only in the index. The total value of the sum will not change if the index i in the third term is replaced by k, yielding a slightly simpler

$$p^2(t) + p^2(t+T) = \sum_{k=1}^{n}\sum_{i=1}^{n} 2^2 a_k a_i \left\{ 2 - 2\,[1 + (-1)^k] \cos\frac{k\pi t}{T} + [1+(-1)^{k+i}] \cos\frac{k\pi t}{T} \cos\frac{i\pi t}{T} \right\}. \tag{A9}$$

The expressions of the form $[1 + (-1)^k]$ that appear in Eq. (A9) are nonzero only for k even. This suggests the following definition:

$$even(k) \equiv \begin{cases} 1; & k \text{ even} \\ 0; & k \text{ odd.} \end{cases}$$

Using the *even* function just defined, squaring Eq. (A9) and substituting it into Eq. (A6) results, after some permutation of the indices, in

$$\begin{aligned} E\{|m_R(t)|^4\} = \frac{1}{T}\int_0^T \sum_{k=1}^{n}\sum_{i=1}^{n}\sum_{m=1}^{n}\sum_{r=1}^{n} a_k a_i a_m a_r \Bigg\{ & 2^6 \\ & - 2^8\, even(k) \cos\frac{k\pi t}{T} \\ & + 2^8\, even(k)\, even(i) \cos\frac{k\pi t}{T} \cos\frac{i\pi t}{T} \\ & + 2^7\, even(k+i) \cos\frac{k\pi t}{T} \cos\frac{i\pi t}{T} \\ & - 2^8\, even(k)\, even(i+m) \cos\frac{k\pi t}{T} \cos\frac{i\pi t}{T} \cos\frac{m\pi t}{T} \\ & + 2^6\, even(k+i)\, even(m+r) \cos\frac{k\pi t}{T} \cos\frac{i\pi t}{T} \cos\frac{m\pi t}{T} \cos\frac{r\pi t}{T} \Bigg\} dt. \end{aligned} \tag{A10}$$

The products of cosines in this equation can be expressed as sums of cosines using the trigonometric identities

$$\cos\alpha \cos\beta = 2^{-1}[\cos(\alpha+\beta) + \cos(\alpha-\beta)],$$

$$\cos\alpha \cos\beta \cos\gamma = 2^{-2}[\cos(\alpha+\beta+\gamma) + \cos(\alpha+\beta-\gamma) + \cos(\alpha-\beta+\gamma) + \cos(\alpha-\beta-\gamma)],$$

and

$$\begin{aligned} \cos\alpha \cos\beta \cos\gamma \cos\phi = 2^{-3} & [\cos(\alpha+\beta+\gamma+\phi) + \cos(\alpha+\beta+\gamma-\phi) \\ & + \cos(\alpha+\beta-\gamma+\phi) + \cos(\alpha+\beta-\gamma-\phi) \\ & + \cos(\alpha-\beta+\gamma+\phi) + \cos(\alpha-\beta+\gamma-\phi) \\ & + \cos(\alpha-\beta-\gamma+\phi) + \cos(\alpha-\beta-\gamma-\phi)]. \end{aligned}$$

Using the additional fact that

$$\frac{1}{T}\int_0^T \cos\frac{k\pi t}{T}\, dt = \delta_k,$$

Equation (A10) can be integrated term by term to yield

$$
\begin{aligned}
E\{|m_R(t)|^4\} = \sum_{k=1}^{n}\sum_{i=1}^{n}\sum_{m=1}^{n}\sum_{r=1}^{n} a_k a_i a_m a_r \Big\{ \; & 2^6 \\
& - 2^8\, even(k)\, \delta_k \\
& + 2^7\, even(k)\, even(i)\, (\delta_{k+i} + \delta_{k-i}) \\
& + 2^6\, even(k+i)\, (\delta_{k+i} + \delta_{k-i}) \\
& - 2^6\, even(k)\, even(i+m)\, (\delta_{k+i+m} + \delta_{k+i-m} + \delta_{k-i+m} + \delta_{k-i-m}) \\
& + 2^3\, even(k+i)\, even(m+r)\, (\; \delta_{k+i+m+r} + \delta_{k+i+m-r} \\
& \qquad + \delta_{k+i-m+r} + \delta_{k+i-m-r} \\
& \qquad + \delta_{k-i+m+r} + \delta_{k-i+m-r} \\
& \qquad + \delta_{k-i-m+r} + \delta_{k-i-m-r}) \Big\} .
\end{aligned}
$$

Since the indices are always positive, some of the delta functions have subscripts that, because they consist only of positive terms, cannot be zero. Eliminating terms containing those delta functions and combining the two terms containing δ_{k-i} gives:

$$
\begin{aligned}
E\{|m_R(t)|^4\} = \sum_{k=1}^{n}\sum_{i=1}^{n}\sum_{m=1}^{n}\sum_{r=1}^{n} a_k a_i a_m a_r \Big\{ \; & 2^6 + 2^6\,[\,2\, even(k)\, even(i) + even(k+i)\,]\, \delta_{k-i} \\
& - 2^6\, even(k)\, even(i+m)\, (\delta_{k+i-m} + \delta_{k-i+m} + \delta_{k-i-m}) \\
& + 2^3\, even(k+i)\, even(m+r)\, (\; \delta_{k+i+m-r} + \delta_{k+i-m+r} \\
& \qquad + \delta_{k+i-m-r} + \delta_{k-i+m+r} \\
& \qquad + \delta_{k-i+m-r} + \delta_{k-i-m+r} \\
& \qquad + \delta_{k-i-m-r}) \Big\} . \qquad \text{(A11)}
\end{aligned}
$$

This can be further simplified by removing some redundant references to the *even* function. For example, consider the first delta function in the above equation. It is nonzero only if $k - i$ is zero. Using symbol $\Longrightarrow$ *implies* for logical implication (if a then b):

$$
\begin{aligned}
k - i = 0 \; & \Longrightarrow \; k - i \; even \\
& \Longrightarrow \; (k \; odd \wedge i \; odd) \vee (k \; even \wedge i \; even) \\
& \Longrightarrow \; k + i \; even .
\end{aligned}
$$

Therefore,

$$
even(k + i)\, \delta_{k-i} = \delta_{k-i} .
$$

Similarly,

$$
k \; even \wedge k \pm i \pm m = 0 \; \Longrightarrow \; i + m \; even,
$$

which, in turn, implies

$$
even(k)\; even(i + m)\; (\delta_{k+i-m} + \delta_{k-i+m} + \delta_{k-i-m}) = even(k)\; (\delta_{k+i-m} + \delta_{k-i+m} + \delta_{k-i-m}) .
$$

The reference to $even(m + r)$ in Eq. (A11) can also be shown to be redundant. Applying these simplifications to Eq. (A11) gives

$$E\{|m_R(t)|^4\} = \sum_{k=1}^{n}\sum_{i=1}^{n}\sum_{m=1}^{n}\sum_{r=1}^{n} a_k a_i a_m a_r \Big\{ 2^6 + 2^6[2\,even(k)\,even(i) + 1]\,\delta_{k-i} - 2^6\,even(k)\,(\delta_{k+i-m}+\delta_{k-i+m}+\delta_{k-i-m}) + 2^3\,even(k+i)\,(\delta_{k+i+m-r}+\delta_{k+i-m+r} + \delta_{k+i-m-r}+\delta_{k-i+m+r} + \delta_{k-i+m-r}+\delta_{k-i-m+r} + \delta_{k-i-m-r})\Big\}. \tag{A12}$$

The Mean of the Squared Amplitude

I now calculate the expected value of the square of the amplitude of the random OQPSK process described by Eq. (19), first with no restrictions on the real baseband pulse function $p(t)$ and then with the $p(t)$ of Eq. (18) considered as a special case of the general result.

The General Result: Real Baseband Pulse Functions

Separate the consideration of the random variable u by formulating the desired moment in terms of a conditional expectation:

$$\{|m_R(t)|^2\} = \frac{1}{T}\int_0^T E\{|m_R(t)|^2 \Big| u\}\,du\,. \tag{A13}$$

Now, calculate that conditional expectation by substituting for $m_R(t)$ from Eq. (19) and factoring all the nonrandom variables (including u, in this context) out of the expectation:

$$E\{|m_R(t)|^2|\,u\} = \sum_k \sum_m E\{\beta_k\beta_m\}\, j^k\, j^{-m}\, p(t - kT - u)\, p(t - mT - u)\,.$$

The baseband pulse function $p(t)$ has been assumed real. Consider the remaining expectation $E\{\beta_k\beta_m\}$. Because the expectation of a product of independent random variables is equal to the product of the expectations of those variables, and because the expectations of each of the $\{\beta_k\}$ are zero,

$$E\{\beta_k\beta_m\} = \delta_{m-k}.$$

Therefore,

$$E\{|m_R(t)|^2 \Big| u\} = \sum_k p^2(t - kT - u).$$

This can now be substituted back into Eq. (A13) and the integration brought inside the summation over k.

$$E\{|m_R(t)|^2\} = \frac{1}{T}\sum_k \int_0^T p^2(t - kT - u)\,du\,.$$

Applying the change of variable $\tau = t - kT - u$ in the integral gives

$$E\{|m_R(t)|^2\} = \frac{1}{T}\sum_k \int_{t-(k+1)T}^{t-kT} p^2(\tau)\,d\tau.$$

It is now clear that the sum over k can be eliminated in favor of infinite limits on the integral.

$$E\{|m_R(t)|^2\} = \frac{1}{T}\int_{-\infty}^{\infty} p^2(\tau)\,d\tau. \tag{A14}$$

Equation (A14) is the general expression for this OQPSK second moment for real baseband pulse functions.

Special Case: Baseband Pulse Functions With Limited Support

For the special case of baseband pulse functions (such as those of Eq. (18)) satisfying the finite support restriction

$$p(t) = 0; \quad |t - T| \geqslant T,$$

the limits of integration can be shrunk to give

$$E\{|m_R(t)|^2\} = \frac{1}{T}\int_0^{2T} p^2(\tau)\, d\tau. \tag{A15}$$

More Special Case: Baseband Pulse Functions as Sums of Raised Cosines

I now evaluate the second moment given by Eq. (A15) for baseband pulse functions described by Eq. (18). Substituting Eq. (18) into Eq. (A15) gives

$$E\{|m_R(t)|^2\} = \frac{1}{T}\int_0^{2T} \sum_{k=1}^{n}\sum_{i=1}^{n} 4a_k a_i \left[1 - \cos\frac{k\pi t}{T}\right]\left[1 \cos\frac{i\pi t}{T}\right] dt.$$

Multiplying the raised-cosine products and converting the product of cosines to a sum of cosines give

$$E\{|m_R(t)|^2\} = \frac{1}{T}\int_0^{2T} \sum_{k=1}^{n}\sum_{i=1}^{n} a_k a_i \left\{ 4 - 4\cos\frac{k\pi t}{T} - 4\cos\frac{i\pi t}{T} + 2\cos\frac{(k+i)\pi t}{T} + 2\cos\frac{(k-i)\pi t}{T}\right\} dt.$$

The integration is over integral multiples of the periods of the cosines, so all the cosine terms disappear in the integration except the last, which has nonzero value only when $k - i = 0$:

$$E\{|m_R(t)|^2\} = \sum_{k=1}^{n}\sum_{i=1}^{n} a_k a_i [2^3 + 2^2\delta_{k-i}]. \tag{A16}$$

While the above form will prove convenient for further manipulation, a more conventional-looking result can be obtained by splitting the sum into two to eliminate the delta function

$$E\{|m_R(t)|^2\} = 8\sum_{k=1}^{n}\sum_{i=1}^{n} a_k a_i + 4\sum_{k=1}^{n} a_k^2,$$

and then factoring the first sum:

$$E\{|m_R(t)|^2\} = 8\left\{\sum_{k=1}^{n} a_k\right\}^2 + 4\sum_{k=1}^{n} a_k^2.$$

The Variance of the Squared Amplitude

The expressions given by Eqs. (A16) and (A12) for the second and fourth moments of the amplitude of the OQPSK process described by Eqs. (19) and (18) can now be combined according to Eq. (A1) to give the variance of the squared amplitude of the process. Squaring the second moment given by Eq. (A16) results in

$$(E\{|m_R(t)|^2\})^2 = \sum_{k=1}^{n}\sum_{i=1}^{n}\sum_{m=1}^{n}\sum_{r=1}^{n} a_k a_i a_m a_r \left\{2^6 + 2^6\delta_{k-i} + 2^4\delta_{k-i}\delta_{m-r}\right\}.$$

Combining this expression with Eq. (A12) in the right-hand side of Eq. (A1) gives

$$\begin{aligned}\mathrm{Var}\{|m_R(t)|^2\} = \sum_{k=1}^{n}\sum_{i=1}^{n}\sum_{m=1}^{n}\sum_{r=1}^{n} a_k a_i a_m a_r \Big\{ & 2^7\, even(k)\, even(i)\,\delta_{k-i} \\ & - 2^4\delta_{k-i}\delta_{m-r} \\ & - 2^6\, even(k)\,(\delta_{k+i-m} + \delta_{k-i+m} + \delta_{k-i-m}) \\ & + 2^3\, even(k+i)\,(\ \delta_{k+i+m-r} + \delta_{k+i-m+r} \\ & \quad + \delta_{k+i-m-r} + \delta_{k-i+m+r} \\ & \quad + \delta_{k-i+m-r} + \delta_{k-i-m+r} \\ & \quad + \delta_{k-i-m-r})\Big\},\end{aligned}$$

which is the desired result: the variance of the squared amplitude of the OQPSK process described by Eqs. (19) and (18).

Appendix B
THE AUTOCORRELATION AND SPECTRAL DENSITY OF AN OQPSK PROCESS

In this appendix I calculate the autocorrelation and spectral density of the OQPSK process given by Eq. (19). The autocorrelation of a complex random process $x(t)$ is defined by

$$R_{xx^*}(t_1, t_2) \equiv E\{x(t_1)x^*(t_2)\}.$$

Applying this definition to the OQPSK random process of Eq. (19) and using a conditional expectation,

$$R_{m_R m_R^*}(t_1, t_2) = \frac{1}{T}\int_0^T E\{m_R(t_1)m_R^*(t_2) \mid u\}\, du\,. \tag{B1}$$

Formulating the conditional expectation from Eq. (19) yields

$$E\{m_R(t_1)m_R^*(t_2) \mid u\} = \sum_k \sum_m E\{\beta_k \beta_m\}\, j^k j^{-m}\, p(t_1 - kT - u)\, p(t_2 - mT - u)\,.$$

But, it is argued in Appendix A that $E\{\beta_k \beta_m\} = \delta_{m-k}$. Therefore,

$$E\{m_R(t_1)m_R^*(t_2) \mid u\} = \sum_k p(t_1 - kT - u)\, p(t_2 - kT - u)\,.$$

Substituting this back into Eq. (B1) produces

$$R_{m_R m_R^*}(t_1, t_2) = \frac{1}{T}\sum_k \int_0^T p(t_1 - kT - u)\, p(t_2 - kT - u)\, du\,.$$

A change of variable $v = t_1 - kT - u$ in the integral gives

$$R_{m_R m_R^*}(t_1, t_2) = \frac{1}{T}\sum_k \int_{t-(k+1)T}^{t-kT} p(v)\, p(v + t_2 - t_1)\, dv\,,$$

which makes it clear that the sum can be eliminated by extending the limits of the integral to infinity:

$$R_{m_R m_R^*}(t_1, t_2) = \frac{1}{T}\int_{-\infty}^{\infty} p(v)\, p(v + t_2 - t_1)\, dv\,.$$

Since t_1 and t_2 appear only in their *difference*, the process $m_R(t)$ is wide-sense stationary. For such processes it is conventional to write the autocorrelation as a function of a single variable representing the difference between the two times. Letting $\tau = t_2 - t_1$ in the above equation and changing the variable of integration back to the more conventional t,

$$R_{m_R m_R^*}(\tau) = \frac{1}{T}\int_{-\infty}^{\infty} p(t)\, p(t + \tau)\, dt\,. \tag{B2}$$

This is the general result for the autocorrelation of an OQPSK process with a real baseband pulse function.

The spectral density of a random process is defined as the Fourier transform of its autocorrelation function. To transform Eq. (B2), first express it as a convolution:

$$R_{m_R m_R^*}(\tau) = \frac{1}{T}\,[p(\tau) \circledast p(-\tau)]\,.$$

Denoting the Fourier transform of $p(\tau)$ by $P(j\Omega)$, the transform of $p(-\tau)$ is just $P(-j\Omega)$. Since $p(\tau)$ is real, $P(j\Omega)$ is conjugate symmetric, i.e., $P(j\Omega) = P^*(-j\Omega)$. The Fourier transform of $p(-\tau)$ is therefore $P^*(j\Omega)$. Since the Fourier transform of the convolution of two functions is just the product of the Fourier transforms of the two functions, the desired spectral density can be written

$$S_{m_R m_R^*}(\Omega) = \frac{1}{T} P(j\Omega) P^*(j\Omega) = \frac{1}{T} |P(j\Omega)|^2.$$

The spectral density $S_{m_R m_R^*}(\Omega)$ is shown as a function of Ω rather than $j\Omega$ to emphasize that when integrated to obtain power it must be with respect to Ω only.

For the baseband pulse functions of interest, those given by Eq. (18), the (bilateral) Laplace transform is given by $P(s) = G(s)F(s)$ where $F(s)$ is given by Eq. (16) or Eq. (26) and where $G(s)$ is the (bilateral) Laplace transform of the gate function $g(t)$ defined in Eq. (5):

$$G(s) = \frac{1 - e^{-2Ts}}{s} = 2T e^{-Ts} \frac{\sinh Ts}{Ts} .$$

The Fourier transform of $p(\tau)$ is obtained by evaluating the Laplace transform $P(s)$ at $s = j\Omega$. Performing the substitution using Eq. (26) for $F(s)$ gives

$$P(j\Omega) = 2T\gamma e^{-j\Omega T} \frac{\sin \Omega T}{\Omega T} \frac{\prod_{k=1}^{m} 1 - \left(\frac{\Omega T}{z_k}\right)^2}{\prod_{k=1}^{n} 1 - \left(\frac{\Omega T}{k\pi}\right)^2} .$$

and, consequently,

$$S_{m_R m_R^*}(\Omega) = \frac{1}{T} |P(j\Omega)|^2 = 4T\gamma^2 \frac{\sin^2 \Omega T}{\Omega^2 T^2} \frac{\prod_{k=1}^{m} \left[1 - \left(\frac{\Omega T}{z_k}\right)^2\right]^2}{\prod_{k=1}^{n} \left[1 - \left(\frac{\Omega T}{k\pi}\right)^2\right]^2} .$$

The above form can be normalized to be independent of the bit interval T by expressing it as a function of a normalized frequency variable $\Omega_T = \Omega T$ rather than a function of Ω. This must be done in such a way that the power in a given frequency interval, obtained by integration of the density, remains unchanged:

$$power(\Omega_1, \Omega_2) = \int_{\Omega_1}^{\Omega_2} S_{m_R m_R^*}(\Omega)\, d\Omega = \int_{\Omega_1 T}^{\Omega_2 T} s_{m_R m_R^*}(\Omega_T)\, d(\Omega_T).$$

Hence,

$$S_{m_R m_R^*}(\Omega_T) = \frac{1}{T} S_{m_R m_R^*}(\Omega),$$

or,

$$S_{m_R m_R^*}(\Omega_T) = 4\gamma^2 \frac{\sin^2 \Omega_T}{\Omega_T^2} \frac{\prod_{k=1}^{m} \left[1 - \left(\frac{\Omega_T}{z_k}\right)^2\right]^2}{\prod_{k=1}^{n} \left[1 - \left(\frac{\Omega_T}{k\pi}\right)^2\right]^2} .$$

DEPARTMENT OF THE NAVY

NAVAL RESEARCH LABORATORY
Washington, D.C. 20375-5000